

Effects of Impurity Elements on Isothermal Grain Growth of Electroplated Copper

Q. Huang (D*,Z

Department of Chemical and Biological Engineering, Center of Materials for Information Technology, University of Alabama, Tuscaloosa, Alabama 35487, USA

The grain growth of electroplated copper films implanted with individual impurity elements were studied with elements implanted separately. Sheet resistance evolution, focus ion beam imaging, and X-ray diffraction were used to characterize the grain growth along time at various annealing temperatures. While the incorporation of oxygen, sulfur, and chlorine impedes the grain growth, the oxygen has the weakest impact and chlorine has the strongest. Fully transformed films with coarse grains were obtained at temperatures up to 400 C. The presence of carbon resulted in a nucleation limited grain growth and the full transformation was not achieved until at 700 C. On the other hand, the presence of chlorine enhanced a preference of grain growth in [111] orientation. This study aims to provide a new perspective of improving grain structures of copper with engineered chemical additives.

© The Author(s) 2018. Published by ECS. This is an open access article distributed under the terms of the Creative Commons Attribution Non-Commercial No Derivatives 4.0 License (CC BY-NC-ND, http://creativecommons.org/licenses/by-nc-nd/4.0/), which permits non-commercial reuse, distribution, and reproduction in any medium, provided the original work is not changed in any

way and is properly cited. For permission for commercial reuse, please email: oa@electrochem.org. [DOI: 10.1149/2.0271807jes]

CC BY-NC-ND

Manuscript submitted February 22, 2018; revised manuscript received March 27, 2018. Published April 21, 2018.

The fabrication of Cu interconnects in semiconductor and microelectronic devices is enabled by a copper electroplating process.¹ One of the reasons why electroplated copper was selected was the so called self-annealing behavior, where the copper grains grow at room temperature.^{2,3} Cu lines with large gains not only typically translates to a lower resistivity of wirings but also often improves the resistance to electromigration or, in other words, the reliability of interconnects.^{4,5} Annealing at a moderately high temperature is typically used to achieve large copper grains. In recent years, as the structures continue to scale, it becomes increasingly difficult for the grain growth to extend into the fine structures, resulting in higher electrical resistance⁶ and lower reliability to electromigration⁵ of the structures. This difficulty has resulted from not only the confined geometry itself⁷ but also the much higher impurity incorporated in the electroplated Cu fine structures. 8,9 Some innovative methods and new materials have been adopted to improve the grain growth and reliability of interconnects. 10-15 While processes and chemistries to lower the impurity incorporation in electroplated copper are of interest, the options are often limited because of the need for specific chemistry and process to achieve the super-conformal filling process. 16-13

The impurity incorporation of electroplated copper is typically modulated with process conditions and organic additives used in the electrolyte. While two of the additive components, suppressor and accelerator, are primarily used to achieve the super-conformal filling of copper in trenches and vias, additional additives, such as so called levelers can be used to provide some control on the morphology and impurity of copper.^{19–21} It is known that a higher impurity level in the electroplated copper typically results in a hindered grain growth across various annealing temperatures.^{9,21,22} However, such observations were often based on studies where different impurity elements including carbon, oxygen, sulfur, and chloride, were incorporated simultaneously with the use of organic additives. Therefore, these impurity elements typically increase or decrease simultaneously.

This letter reports a study attempting to separate the effects of different elemental impurities on the copper grain growth. While the high impurity incorporation in copper lines impedes the grain growth into fine structures, this study aims to answer the questions if any of the impurity elements dominate such effect, and, if so, which element or elements should be mitigated or avoided in the design of chemistry and process.

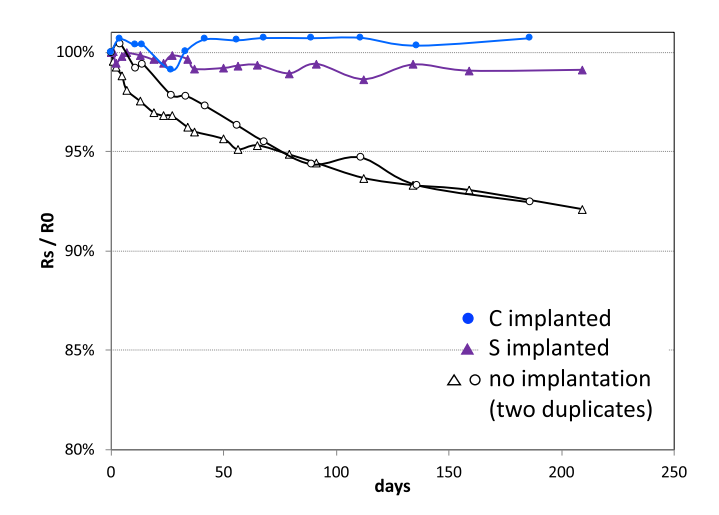


Figure 1. Normalized sheet resistance evolution of as deposit copper films and films implanted with sulfur and carbon at room temperature.

Experimental

Silicon wafer coupons of about 6 cm \times 6 cm size with physical vapor deposited 10 nm TaN, 16 nm Ta, and 20 nm Cu layers were used to electroplate 180 nm copper films. The electrolyte comprises 0.6 M CuSO₄, 0.1 M H₂SO₄, 1.4 mM HCl. A commercial copper damascene additive, Nanofill from Dow Chemical, was used. The specifications of the chemistry are not critical to this study as long as the impurity in deposited films is significantly lower than the dose used in implantation (further discussed in Figure 1). A typical commercial copper chemistry for damascene copper would satisfy this requirement. The wafer coupons in this study were mounted on to a rotating disc electrode with front contacts. A two-electrode cell was used with the coupons as cathode and a copper foil as anode. Deposition was carried out at a rotation rate of 30 rpm and a current density of -20 mA/cm² for 30 seconds. This corresponds to a film thickness of 180 nm at a pre-determined efficiency of 80%, resulting in a total copper film thickness of 200 nm. The sheet resistance of electrodeposited copper was measured with a 4-point probe immediately after plating. Point-to-point variation of less than 6% were typically observed within the central 4 cm × 4 cm portion of the wafers. All further studies were carried out using these centre portions.

Ion implantation was used to dope predetermined amounts of various impurity elements into different wafers. The free software SRIM

^{*}Electrochemical Society Member.

^zE-mail: qhuang@eng.ua.edu

Table I. Dose and conditions for multiple step implantation of different elemental impurities. The area doses are the conditions used in ion implantation. The volumetric doses are calculated from the area doses and film thickness, which is 200 nm or 2E-5 cm. Volumetric doses are included here to allow easier comparison with SIMS data in literature.

		C	O	S	Cl-low	Cl-high
volumetric o	dose (atom/cm ³)	1×10^{20}	3×10^{19}	3×10^{19}	3×10^{19}	1×10^{20}
area dose used (atom/cm ²)		2×10^{15}	6×10^{14}	6×10^{14}	6×10^{14}	2×10^{15}
step 1	area dose (atom/cm ²)	2.4×10^{14}	7×10^{13}	1×10^{14}	9×10^{13}	3×10^{14}
•	energy (kV)	20	30	40	40	40
step 2	area dose (atom/cm ²)	2.4×10^{14}	1.6×10^{14}	1×10^{14}	9×10^{13}	3×10^{14}
•	energy (kV)	50	80	100	100	100
step 3	area dose (atom/cm ²)	1×10^{15}	3×10^{14}	4×10^{14}	4.2×10^{14}	1.4×10^{15}
•	energy (kV)	90	120	220	220	220
step 4	area dose (atom/cm ²)	5.2×10^{14}	7×10^{13}	NA	NA	NA
	energy (kV)	120	150			

was used to simulate and predict the implantation depth profile across the film stacks. As shown in Figure S-1 in supporting materials, multiple implantation steps with different accelerating energy were used to achieve a relatively uniform distribution of the implanted elements across the whole thickness of copper film. Details of the doses and implantation conditions were listed in Table I. Because of the so-called matrix effect of the host materials, impurity quantification by SIMS analysis requires calibration with standards. Copper films with a fixed high dose of various impurities were used as standards in our study. In other words, implantation doses were considered to be accurate. Therefore, impurity concentration profiles in the implanted films were not analyzed again using SIMS.

Four elements, carbon, oxygen, sulfur, and chlorine, are studied. A dose of 3E19 atom/cm³ was used for sulfur and 1E20 atom/cm³ for chlorine. While carbon and oxygen levels in fine lines were not available from literature because of the presence of dielectric materials in those studies, they are typically comparable with chlorine and sulfur, respectively, in plated thin films.²² Therefore, a dose of 3E19 atom/cm³ for oxygen and 1E20 atom/cm³ for carbon were used in this study. An additional study with chlorine implantation at a dose of 3E19 atom/cm³ was included to allow a direct comparison on the effects of different elements. These doping concentrations are much higher than the impurity in a typical damascene copper film. However, the purpose of this study is to use thin films with an impurities level similar to the lines to investigate the grain growth behavior in the lines. The doping concentrations used here represent the typical impurity levels in narrow lines in interconnect structures, which are typically 100 times higher than in thin films or the overburden region.⁸,

Implanted wafers were cleaved into 2 cm × 2 cm coupons for further studies. Annealing were carried out in a rapid thermal annealing furnace. A slightly reducing ambient (forming gas) was used to avoid film oxidation at high temperature. The ramping rate was at least 10 C/sec and the coupons were maintained at various elevated temperatures for different times. All coupons used in the studies were checked with sheet resistance. As shown in Figure S-1 in Supporting Materials, measurements were repeated for 50 as-plated coupons and an average sheet resistance of 0.108 ohm/sq was observed, corresponding to a resistivity of 2.16E-8 ohm-m for 200 nm thick films. This corresponds to a resistivity of 1.73E-8 ohm-m with a 20% resistance drop from as-plated films, consistent with bulk copper resistivity. More importantly, a standard deviation of 3.1% was observed for the 50 samples, suggesting a thickness consistency across the films used in this study. This is expected to mitigate the variation in grain growth due to the variation in film thickness.14

Also presented in Figure S-1 are the sheet resistance of copper films with different implantation. Ten films were measured for each implantation condition, where a standard deviation below 3.5% was observed. In addition, implantation increases the sheet resistance of films, regardless of the species and doses of implantation. However, the resistance upon oxygen and chlorine implantation is less than 3% while the increases were 5.7% and 10.7% for 3E19 atom/cm³ sulfur and 1E20 atom/cm³ carbon. While ion implanta-

tion can interrupt large crystal grains and cause defects in crystalline materials, the as-deposit copper films were nano-crystalline and no grain refining was expected upon implantation. This is confirmed with the full width at half maximum for XRD peaks summarized in Table S-2 in Supporting Materials, where no peak broadening was observed upon implantation. The room temperature Gibbs energy of formation of copper compounds are -147, -138, and -84.5 kJ/mol for CuCl, Cu₂O and Cu₂S, respectively,²³ suggesting Cu₂S is the least stable among the three. In addition, no stable copper carbides are expected to form spontaneously at normal conditions.²⁴ Therefore, it is evident that elements that form strong bonds with copper atoms, Cl and O, result in less increase in resistance, suggesting that the resistance increase upon implantation is probably related to the scattering on free dopant atoms in copper host.

A four-point probe was used for all the sheet resistance measurements. A Bruker D8 X-ray diffractometer was used for the crystallographic characterization of films. A FEI focus ion beam (FIB) workstation was used to acquire top-town images of the films, where grains were revealed due to the channelling effect of ion. All coupons were stored under -40°C with dry ice to avoid grain growth at room temperature before annealing studies.

Results and Discussion

The self-annealing of copper films at room temperature was first monitored by measuring the sheet resistance. Figure 1 shows the normalized resistance of films with and without sulfur and carbon implantation. A resistance drop of 7 to 8% was observed after about 6 months for films without implantation. While this self-annealing was slow, this is not unexpected because of the thin thickness of films. ¹⁴ On the other hand, the two films implanted with carbon and sulfur showed little to no resistance drop, consistent with the retarded grain growth with the presence of higher impurity concentrations.

As-plated copper films are equivalent to the overburden region above copper lines in patterned wafers, where the impurity level is much lower. A measurement with time-of-fly secondary ion mass spectroscopy (TOF-SIMS) was performed for a copper film plated with the same chemistry at the same condition. The concentrations of sulfur and chlorine in the as-plated copper film were 4E17 and 4E18 atom/cm³, respectively. These values are significantly lower than the doses of implantation, 3E19 and 1E20, respectively. Therefore, the implanted elements were expected to dominate the impacts on grain growth.

Figure 2 shows the normalized resistance evolution of the same films with different implanted elements upon annealing at various elevated temperatures for up to 60 minutes. While the un-doped film showed about 15% resistance drop after annealing at 100 C for an hour, it showed full recrystallization, i.e. a resistance drop beyond 20% after only 5 minutes annealing at 150 C or above. A slightly greater resistance drop was observed upon annealing at higher temperatures such as 300 C and 400 C, suggesting a further grain growth at

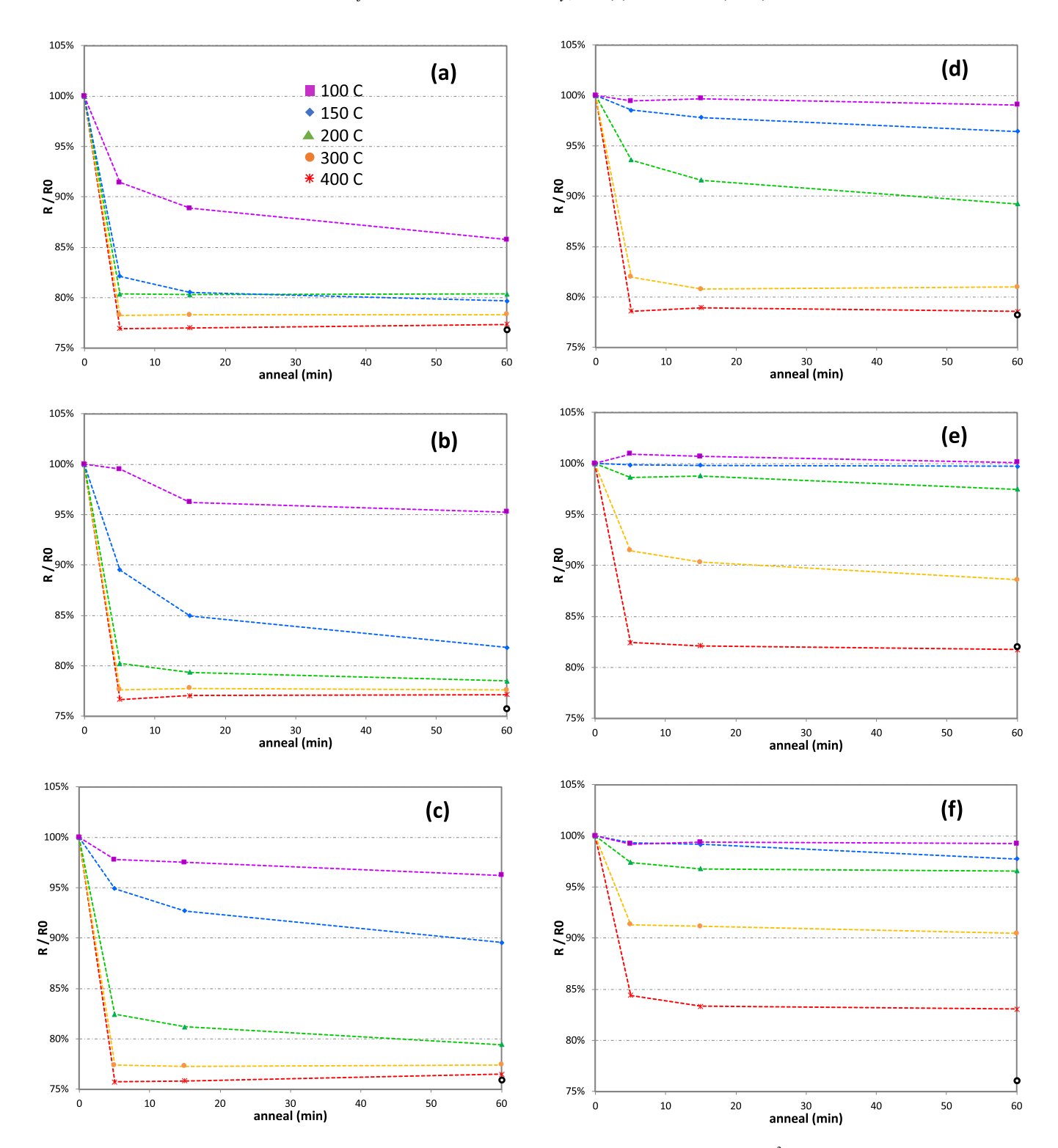


Figure 2. Normalized sheet resistance evolution of (a) as deposit copper films and films implanted with 3E19 atom/cm³ (b) oxygen, (c) sulfur, (d) chlorine, and 1E20 atom/cm³ (e) chlorine and (f) carbon at (ν) 100, (ν) 150, (σ) 200, (λ) 300, and (T) 400 C. Film resistance after annealing at 700 C is labeled as (o) for comparison.

higher temperatures. However, this resistance drop saturated at 400 to 500 C, where 22% drop was observed. Annealing at 700 C did not further change the resistance. With an average resistivity of as-plated film at 2.16E-8 ohm-m (discussed in Experimental section), this corresponds to a bulk copper resistivity of 1.67E-8 ohm-m and suggests that the copper grains in the un-doped copper are fully grown after annealing.

Figures 2b to 2d show the same resistance evolution for films with 3E19 atom/cm³ oxygen, sulfur, and chlorine, respectively. It is evident that, at this doping concentration, chlorine showed the most pronounced suppression effect on grain growth and oxygen the least. For example, the films doped with oxygen, sulfur and chlorine showed 18%, 10% and 4% resistance decrease, respectively, after annealing at 150 C for 60 minutes. This trend was observed at other annealing

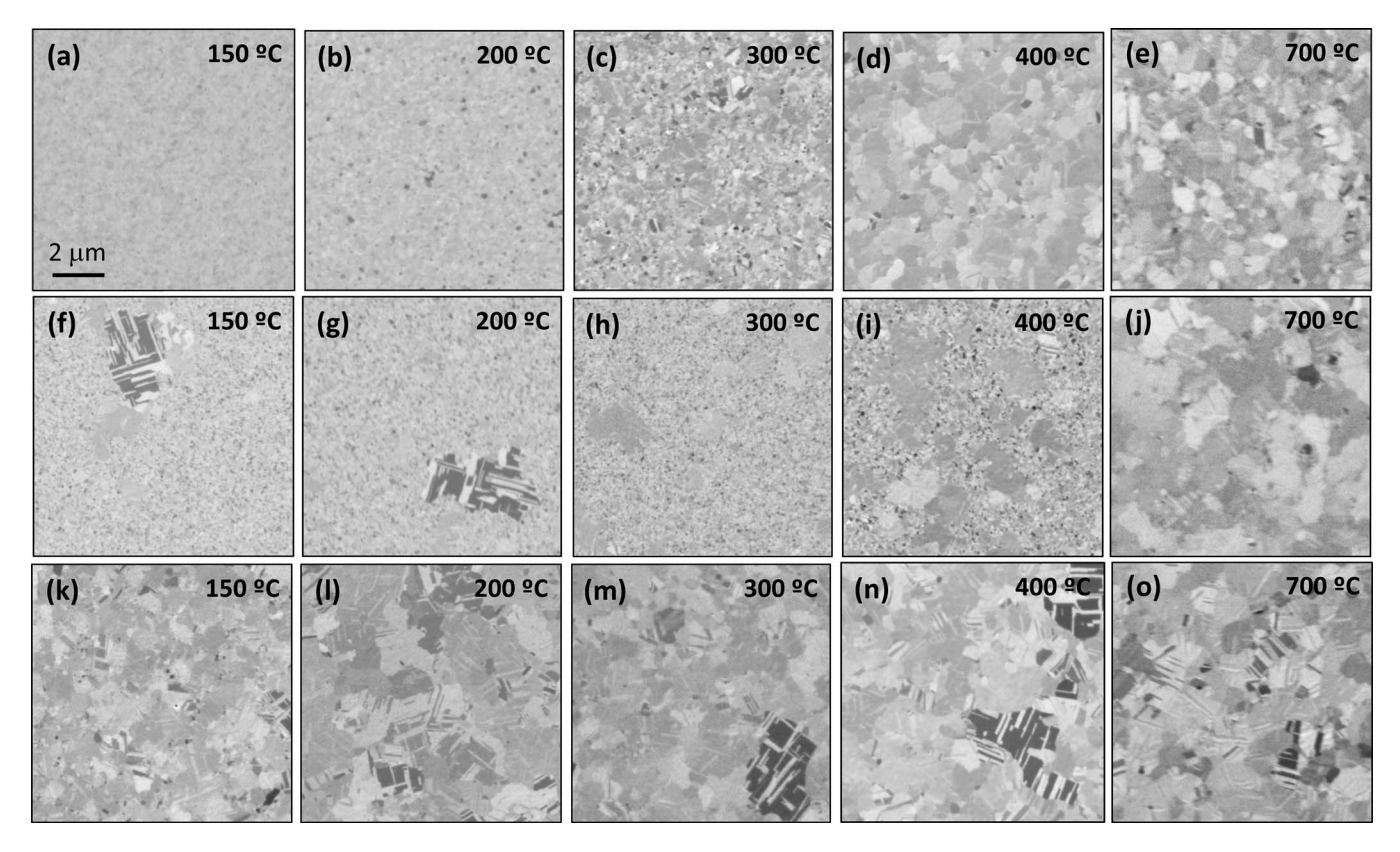


Figure 3. Top down focus ion beam (FIB) images ($10 \mu m \times 10 \mu m$) of copper films implanted with 1E20 atom/cm³ (a-e) chlorine; (f-j) carbon and (k-o) as deposited copper films annealed at various temperatures for 1 hour.

temperatures as well. On the other hand, Figures 2e and 2f show a comparison between chlorine and carbon at a higher doping level of 1E20 atom/cm³. First, an increase in chlorine concentration resulted in a more pronounced inhibition on the resistance drop. Moreover, carbon and chlorine had comparable suppression effects on the copper resistance drop. The resistance drop below 200 C were negligible for both elements. Both elements resulted in a resistance drop of about 10% and 17% for annealing at 300 and 400 C, respectively. In addition, the resistance drops or grain growth at these temperatures seemed to be very fast, where the resistance stabilized after 5-minute annealing.

While the sheet resistance evolutions were similar between carbon and chlorine at the high doping level, the grain growth behaviors were drastically different between the two. Figure 3 shows the top down FIB images of the films annealed at various temperatures for 60 minutes. No coarse grains were observed for chlorine (1E20 atom/cm³) doped films annealed at up to 150 C. While grains were observed after annealing at 300 C, the grains were discontinuous. After annealing at 400 C, the film was found to have completely transformed to coarse grains with a grain size between about 0.5 to 1 um. Contrarily, nucleation of grains was observed in the film doped with carbon even at an annealing temperature as low as 100 C. Grains were able to grow up to a few microns at such a low temperature. However, the density of these coarse grains was extremely low and the change in sheet resistance in Figure 2f was negligible. Twin structures were often observed in the coarse grains formed at low temperature. As the annealing temperature increased, more nuclei of grains formed, but no increase of grain size was observed. The film was not completely converted into coarse grains even after a 60-minute annealing at 400 C.

The FIB images of the as-plated film without implantation were also included in Figure 3 for comparison, where fully transformed copper films with coarse grains were observed at 150 C. The comparison suggests that the presence of 1E20 atom/cm³ chlorine mainly impeded the grain nucleation at low temperature (below 200 C). However, an

almost instantaneous nucleation at high nucleation density was observed at high temperature and a uniform grain size was achieved at 400 C. The driving force for abnormal grain growth is known to relate to the ratios between the size, boundary energy and mobility of the particular grain and the average of matrix.²⁵ In the case of chlorine doped films, the instantaneous nucleation at high temperature resulted in a uniform size of coarse grains and mitigates the driving force of further grain growth. This was consistent with the fact that resistance drop in Figure 2e was achieved only after 5-minute annealing and no further change was observed afterwards. This hypothesis was also confirmed by the grain structure observed after annealing at 700 C shown in Figure 3e, which was similar to 400 C.

On the other hand, while coarse grain nuclei managed to form at low temperatures despite of the presence of a high carbon concentration, the number of nuclei was very limited compared with films without dopant. More importantly, this strong retardation of nucleation was observed even at much higher temperatures of 300 and 400 C. Because of this pronounced inhibition on nucleation, the majority of as-deposited fine grains remained unchanged and resulted in a much smaller average grain size of matrix. Therefore, the nucleation and growth of coarse grains continued due to the large ratio between the sizes of large and fine grains, as observed in Figures 3h and 3i. On the other hand, abnormal grain growth is also limited by a maximum grain size ratio, which depends on the other factors such as grain mis-orientation.^{25–27} While the mis-orientation is hard to estimate because of the random orientations of as-deposited fine grains, this maximum size ratio is expected to limit the final size that a grain can grow. The copper films were not fully transformed into coarse grains even at 400°C because of a limited number of nuclei and a limited maximum size of each grain. While nucleation and growth of new grains can occur because of the presence of fine grains, this was not observed with annealing at the same temperature for longer time. The sheet resistance measurements in Figure 2f also showed that the resistance dropped during the first 15 minutes and no further drop was

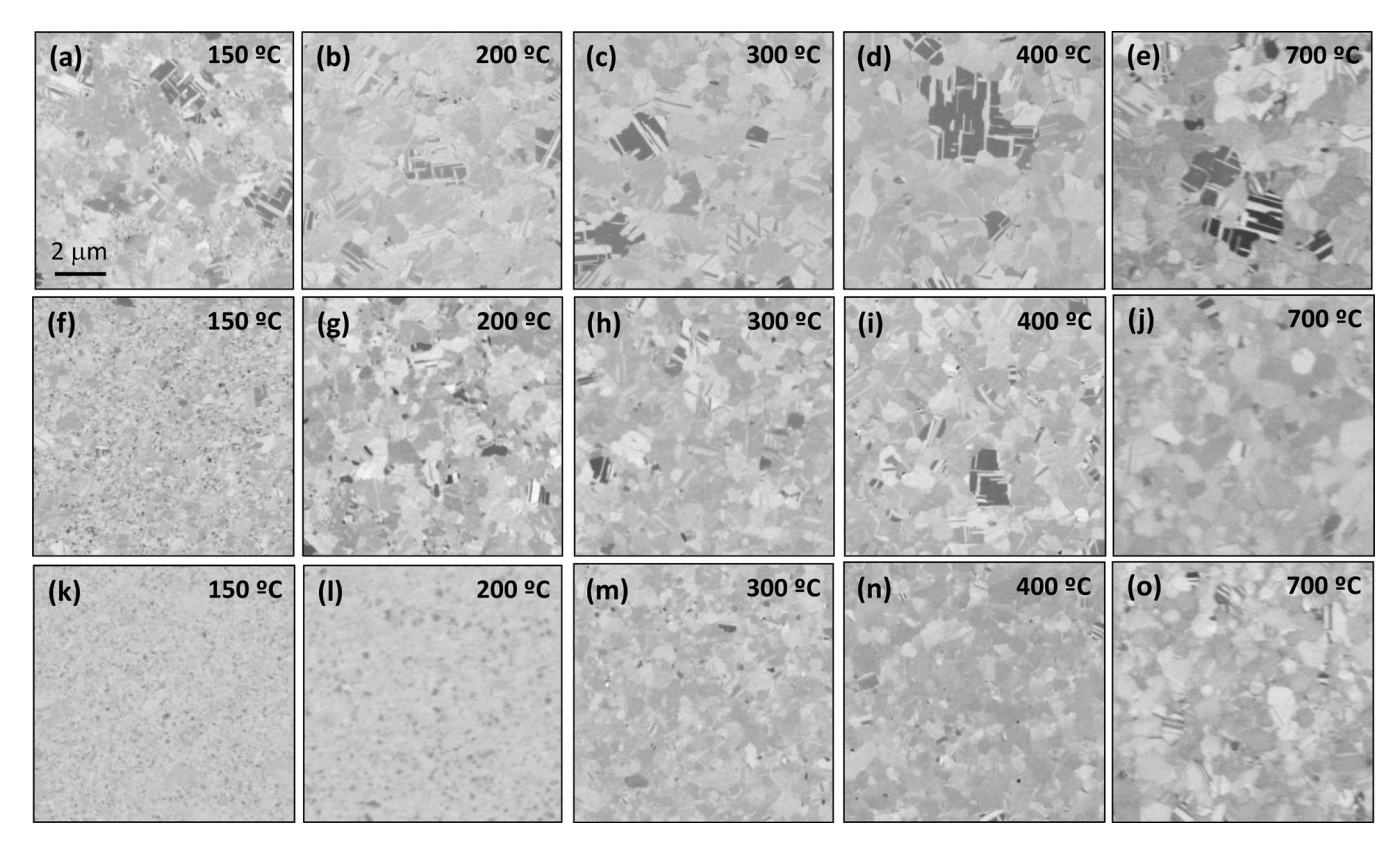


Figure 4. Top down FIB images ($10 \, \mu m \times 10 \, \mu m$) of copper films implanted with 3E19 atom/cm³ (a-e) oxygen; (f-j) sulfur and (k-o) chlorine annealed at various temperatures for 1 hour.

observed for annealing for longer time. Only when a higher temperature was used were further nucleation of grains and further resistance drop achieved. As shown in Figure 3j, a film with fully transformed coarse gains was obtained at a high temperature of 700 C. This is also consistent with Figure 2f, where a further decrease in sheet resistance from 17% at 400 C to 22% at 700 C was observed.

Figure 4 shows the FIB images of films doped with 3E19 atom/cm³ oxygen, sulfur and chlorine, respectively. While all the three impurity elements inhibit the nucleation and growth of copper grains at 150 C, oxygen shows the least pronounced inhibition and chlorine the most. This observation is consistent with the sheet resistance evolution presented in Figure 2. In addition, the more pronounced inhibition effect at low temperature by chlorine resulted in a more instantaneous nucleation of gains at high temperature. In other words, the grain sizes were more uniform in the film with chlorine than sulfur and oxygen.

No significant difference was observed in copper grain size between the cases of 3E19 atom/cm³ chlorine in Figures 4n and 1E20 atom/cm³ chlorine in Figure 3d. However, the resistance drops were 21% and 18% for the two cases after annealing at 400 C, respectively. As shown in Table S-1, the absolute values of film resistance also confirmed a 5% higher resistivity for the film with high chlorine dopant. Furthermore, we know from Table S-1 that the sheet resistance showed no increase upon Cl implantation. Therefore, this higher resistivity of annealed copper films with high dose of Cl is believed to result from a synergistic combination of the high Cl level and the limited grain growth. On the other hand, all other dopants (O, S, C) resulted in a resistance drop of about 24% and similar sheet resistance value at 700 C, which not only is consistent with a fully transformed grain structure but also suggest a negligible ionic effect between copper and these elements after 700 C anneal. It is interesting to note that the impacts of 1E20 atom/cm3 chlorine and carbon were opposite with regard to as-implanted and annealed films. Chlorine does not have much impact on the as-implanted film, but it results in a higher resistivity after annealing. Contrarily, carbon increased film resistance by

10.7% upon implantation but it does not have much impact after 700 C anneal. A detailed atomic probe analysis of films before and after annealing would be needed to understand the out-gas, the distribution of elements, and the mechanism of such opposite impacts.

X-ray diffraction was also carried out for the films and the spectra are presented in Figure S-2 in Supporting Materials. The heights and widths (full width at half maximum, FWHM) of the [111] reflection peak, as well as the height ratio between [111] and [200] peaks, both normalized with the measurement before annealing are summarized in Table II. It is evident that the FWHM drops significantly upon 150 C annealing for copper films without implantation and no further decrease was observed at higher temperatures, indicative of full grain growth at 150 C. Films with oxygen and sulfur implantation showed peak narrowing at 150 C but such decrease didn't stabilize until 200 C. This stabilization temperature further increased to 300 C for chlorine at the same doping level. Such stabilization was not observed up to 400 C for carbon and chlorine at a higher implantation concentration. While an accurate estimation of grain size could not be calculated because of the intrinsic peak widening and the thin thickness of the film, the relationship between FWHM and temperatures is consistent with the observation on sheet resistance and FIB observation. The peak height is typically of less of importance due to the instrumental variation. However, all the XRD measurements were performed in one batch of experiments and the relationship between peak height and annealing temperature also show a similar trend. For example, the [111] peak height increased 4 times after 150 C annealing and did not significantly increase any further at high temperature for copper films without implantation. On the other hand, films with chlorine implantation showed steady and slow increase of the peak height along with the annealing temperatures.

Another interest observation is that the impurity species have an influence on the preferred orientation for grain growth. The [111] and [200] orientations grew simultaneously in copper films without implantation or implanted with oxygen and carbon, resulting in a

Table II. Normalized [111] peak width, [111] peak height, and the [111]/[200] height ratio from XRD spectra of copper films implanted with
different elemental impurities and annealed at different temperatures normalized with as the deposited film.

normalized [111] FWHM	none	O	S	Cl-low	Cl-high	C
before annealing	1	1	1	1	1	1
150 C, 60 min	0.74	0.82	0.79	0.94	0.97	0.94
200 C, 60 min	0.74	0.74	0.74	0.86	0.97	0.94
300 C, 60 min	0.74	0.74	0.74	0.78	0.91	0.89
400 C, 60 min	0.74	0.71	0.74	0.78	0.84	0.78
normalized [111] height	none	O	S	Cl-low	Cl-high	C
before annealing	1	1	1	1	1	1
150 C, 60 min	4.23	3.79	2.99	2.02	2.00	1.97
200 C, 60 min	3.71	4.24	3.82	2.62	1.96	1.89
300 C, 60 min	4.1	4.54	4.59	3.78	2.82	2.61
400 C, 60 min	5.47	5.62	5.48	5.48	5.00	4.69
normalized [111] / [200]	none	O	S	Cl-low	Cl-high	C
before annealing	1	1	1	1	1	1
150 C, 60 min	1.30	1.06	2.16	1.28	1.18	0.49
200 C, 60 min	0.73	1.23	1.40	1.82	1.18	0.97
300 C, 60 min	1.09	1.22	1.96	1.86	1.99	0.70
400 C, 60 min	1.11	1.13	1.89	2.36	2.64	1.21

constant ratio between the two orientations regardless of the annealing temperature. However, the presence sulfur caused a slightly preferred growth in [111] orientation and resulted in a higher [111]/[200] ratio as grain transformation proceeded. This preference was even much more pronounced for chlorine impurity, resulting in a highest [111]/[200] ratio regardless of the implantation dose used for the study.

While the resistance measurements reflect the grain growth in the film, the true volumetric fraction of transformed portion can be calculated based on the ratio between resistance drop and the maximum drop when the entire film is transformed into coarse grains. Table III presents the calculated volumetric fractions of coarse grains with the maximum drop estimated from films annealed at 700 C. The well-known Avrami relationship²⁸ describes an exponential relationship between this volume fraction and annealing time at the early stage of 3-D abnormal grain growth. However, the recrystallization at high temperatures was very rapid and full transformation was often obtained upon annealing for short time. The early stage of the transformation could not be captured. On the other hand, grain growth rarely occurred at low temperatures and very low volume fraction was observed even after 60 min. Only at an intermediate temperature did the volume fraction significantly increase along the annealing time. Cases where the volume fraction increased more than 15% between 5 and 60 min were highlighted and in bold fonts in Table III. It is evident that such temperatures highly depend on the speciation and concentration of impurity. Almost all of these cases still showed significantly faster change within the first 5 minutes, suggesting that the abnormal grain growth in copper films doped with oxygen, sulfur and chlorine consists of a fast nucleation step and a slow grain growth step.

On contrary, the volume fraction increase was less than 7% between 5 and 60 min for films implanted with carbon for all the temperatures studied. Although the transformed fraction was small, this fraction did not significantly grow with time. This is consistent with the afore discussion that the abnormal grain growth was limited by the nucleation of the grains and such grains reached the maximum grain size rapidly. The film with carbon impurity could not be fully transformed at 400 C. While chlorine impurity was also found to significantly hinder the grain growth, full transformation was observed at temperatures up to 400 C.

Conclusions

The impacts of the impurity elements of Carbon, Oxygen, Sulfur and Chlorine, on the grain growth behavior of electroplated copper films were studied with the elements implanted separately. When copper films were implanted with a same concentration of oxygen, sulfur and chlorine, chlorine showed the most pronounced inhibition on the grain growth while oxygen showed the least. This inhibition effect of chlorine becomes further enhanced at a higher incorporation level.

Table III. Volumetric fraction of transformed portion of copper films implanted with different elemental impurities and annealed at different temperatures for different time. Highlighted in green in bold fonts are cases where at least additional 15% of volume fraction was observed between 5 and 60 min.

volume fraction		None	O	S	Cl-low	Cl-high	C
400 C	5 min	100.0%	97.3%	100.8%	97.4%	87.8%	64.9%
	15 min	99.7%	95.7%	100.4%	95.7%	89.5%	69.4%
	60 min	98.2%	95.3%	97.6%	97.4%	91.2%	70.7%
300 C	5 min	94.4%	93.2%	93.9%	81.9%	42.7%	36.3%
	15 min	94.2%	92.6%	94.4%	87.4%	48.5%	36.9%
	60 min	94.1%	93.3%	93.8%	86.4%	57.0%	39.8%
200 C	5 min	85.2%	82.5%	73.0%	29.2%	6.7%	10.9%
	15 min	85.5%	86.0%	78.1%	38.3%	6.1%	13.5%
	60 min	85.2%	89.7%	85.5%	48.9%	12.7%	14.3%
150 C	5 min	77.5%	43.7%	21.1%	6.7%	0.7%	2.9%
	15 min	84.4%	62.7%	30.4%	10.0%	1.0%	3.4%
	60 min	88.3%	75.8%	43.4%	16.3%	1.4%	9.4%
100 C	5 min	37.2%	2.1%	9.2%	2.5%	-4.6%	3.3%
	15 min	48.3%	15.8%	10.3%	1.5%	-3.3%	2.6%
	60 min	61.8%	19.7%	15.7%	4.3%	-0.5%	3.3%

Furthermore, a preference in grain growth suppression in [200] orientation over [111] was observed in presence of chlorine impurity regardless of its concentration. While carbon showed similar degree of inhibition on grain growth as chlorine at a same high concentration, the behaviors of grain growth are completely different. The grain growth of copper films doped with oxygen, sulfur and chlorine all appear to consist of the two steps, a fast nucleation and a slow growth. While such steps are observed at different temperatures for different impurity elements or for different concentrations, full grain growth was achieved at temperatures up to 400 C for all cases. On the other hand, the nucleation of coarse grain in copper film doped with carbon was so suppressed that the grain growth appears relatively fast across all the temperature studied. Full grain growth was not obtained until a much high temperature of 700 C. From the application point of view, chemistries and processes that allow the fabricated copper interconnect structures with significantly lower incorporation of carbon will be beneficial for applications where large grains are

Acknowledgment

National Science Foundation is acknowledged for support through grant CMMI-1662332. The Microfabrication Facility and Central Analytical Facility at University of Alabama and the Georgia Tech Research Corporation are acknowledged for fabrication of substrates, Microscopic characterization, and SIMS analysis.

ORCID

Q. Huang https://orcid.org/0000-0002-1391-6531

References

- P. Andricacos, C. Uzoh, J. Dukovic, J. Horkans, and H. Deligianni, *IBM Journal of Research and Development*, 42, 567 (1998).
- T. Ritzdorf, L. Graham, S. Jin, C. Mu, and D. Fraser, Proceedings of Proceedings of the IEEE 1998 International Interconnect Technology Conference, pp. 166, 1998.
- C. Cabral, P. C. Andricacos, L. Gignac, I. C. Noyan, K. P. Rodbell, T. M. Shaw, R. Rosenberg, J. M. E. Harper, P. W. DeHaven, P. S. Locke, C. Uzoh, and S. J. Klepeis, *Proceedings of Advanced Metallization Conference*, Colorado Spring, CO, 1998.
- J. M. E. Harper, C. Cabral, P. C. Andricacos, L. Gignac, I. C. Noyan, K. P. Rodbell, and C. K. Hu, *Journal of Applied Physics*, 86, 2516 (1999).

- C. K. Hu, L. Gignac, B. Baker, E. Liniger, R. Yu, and P. Flaitz, *Proceedings of IEEE 2007 International Interconnect Technology Conference*, pp. 93, Burlington, CA, 2007.
- K. Barmak, A. Darbal, K. J. Ganesh, P. J. Ferreira, J. M. Rickman, T. Sun, B. Yao, A. P. Warren, and K. R. Coffey, *Journal of Vacuum Science & Technology A*, 32, 061503 (2014).
- W. Zhang, S. H. Brongersma, N. Heylen, G. Beyer, W. Vandervorst, and K. Maex, Journal of The Electrochemical Society, 152, C832 (2005).
- J. Kelly, T. Nogami, O. Van der Straten, J. Demarest, J. Li, C. Penny, T. Vo, C. Parks, P. DeHaven, and C.-K. Hu, *Journal of The Electrochemical Society*, 159, D563 (2012).
- Q. Huang, A. Avekians, S. Ahmed, C. Parks, B. Baker-O'Neal, S. Kitayaporn, A. Sahin, Y. Sun, and T. Cheng, *Journal of The Electrochemical Society*, 161, D388 (2014).
- C. K. Hu, L. M. Gignac, E. Liniger, E. Huang, S. Greco, P. McLaughlin, C. C. Yang, and J. J. Demarest, *Proceedings of Proceedings of 10th International Workshop on Stress-Induced Phenomena in Metallization*, pp. 3, 2009.
- C. Christiansen, B. Li, M. Angyal, T. Kane, V. McGahay, Y. Y. Wang, and S. Yao, Proceedings of Proceedings of 2011 IEEE International Reliability Physics Symposium (IRPS), pp. 3E.3.1, 2011.
- C. K. Hu, J. Ohm, L. M. Gignac, C. M. Breslin, S. Mittal, G. Bonilla, D. Edelstein, R. Rosenberg, S. Choi, J. J. An, A. H. Simon, M. S. Angyal, L. Clevenger, J. Maniscalco, T. Nogami, C. Penny, and B. Y. Kim, *Journal of Applied Physics*, 111, 093722 (2012).
- C. Christiansen, B. Li, M. Angyal, T. Kane, V. McGahay, Y. Y. Wang, and S. Yao, Proceedings of Reliability Physics Symposium (IRPS), 2012 IEEE International, pp. 5E. 1.1-5E. 1.4, 2012.
- Q. Huang, B. C. Baker-O'Neal, C. Cabral, E. Simonyi, V. R. Deline, and M. Hopstaken, *Journal of The Electrochemical Society*, 160, D3045 (2013).
- C. Cabral Jr, J. P. Gambino, Q. Huang, T. Nogami, and K. P. Rodbell, US Pat. No. 8,492,897 (2014).
- T. P. Moffat, J. E. Bonevich, W. H. Huber, A. Stanishevsky, D. R. Kelly, G. R. Stafford, and D. Josell, *Journal of The Electrochemical Society*, 147, 4524 (2000).
- W. Zhang, S. H. Brongersma, T. Conard, W. Wu, M. Van Hove, W. Vandervorst, and K. Maex, *Electrochemical and Solid-State Letters*, 8, C95 (2005).
- A. C. West, S. Mayer, and J. Reid, *Electrochemical and Solid-State Letters*, 4, C50 (2001).
- J. D. Reid, E. Webb, J. Sukamto, Y. Takada, and T. Archer, Proceedings of Proceedings of International Symposium on Electrochemical Processing in ULSI and MEMS, pp. 184, San Antonio, TX, 2005.
- J. Sukamto and J. Reid, Proceedings of Proceedings of International Symposium on Electrochemical Processing in ULSI and MEMS, pp. 96, San Antonio, TX, 2005.
- J. D. Reid and J. Zhou, Proceedings of 209th ECS Meeting International Symposium on Electrochemical Processing in ULSI and MEMS 2, pp. 77, Denver, CO, 2007.
- Q. Huang, B. C. Baker-O'Neal, C. Parks, M. Hopstaken, A. Fluegel, C. Emnet, M. Arnold, and D. Mayer, *Journal of The Electrochemical Society*, 159, D526 (2012).
- 23. I. Barin, Thermochemical data of pure substances, VCH, Weinheim, Germany (1995).
- 24. S. R. Shatynski, Oxidation of Metals, 13, 105 (1979).
- 25. F. Humphreys, *Acta Materialia*, **45**, 4231 (1997).
- 26. F. Humphreys, Acta materialia, 45, 5031 (1997).
- 27. M. Hillert, Acta metallurgica, 13, 227 (1965).
- 28. J. W. Christian, The theory of transformations in metals and alloys, Newnes, (2002).